Research Square

Preprints are preliminary reports that have not undergone peer review.
They should not be considered conclusive, used to inform clinical practice,
or referenced by the media as validated information.

Comparative numerical assessment of SPH, EFG, and SPG methods for orthogonal cutting of steel

Sherzod Ibodulloev

sherzod_uzmu@inbox.ru

Tashkent Institute of Irrigation and Agricultural Mechanization Engineers (TIIAME)

Umarkhon Turaev

Samarkand State University

correspondence

Keywords: metal cutting, mesh-free methods, SPH, EFG, SPG, Johnson–Cook model, LS-DYNA

Posted Date: May 14th, 2026

DOI: https://doi.org/10.21203/rs.3.rs-9633326/v2

License: This work is licensed under a Creative Commons Attribution 4.0 International License.
Read Full License

Additional Declarations: No competing interests reported.

Version of Record: A version of this preprint was published at Continuum Mechanics and Thermodynamics on October 6th, 2026. See the published version at https://doi.org/10.1007/s00161-026-01530-z.

Comparative numerical assessment of SPH, EFG, and SPG methods for orthogonal cutting of steel

IBODULLOEV SH.R[A,B] , TURAEV U. M[C]

a) Tashkent Institute of Irrigation and Agricultural Mechanization Engineers (TIIAME), Tashkent, Uzbekistan
b) National University of Uzbekistan, Tashkent, Uzbekistan
Scopus ID: 57982866900, **Email:** sherzod_uzmu@inbox.ru
c) Samarkand State University, Samarkand, Uzbekistan
email: umarxonturayev17@gmail.com

Abstract

This study presents a comparative analysis of three mesh-free methods—Smoothed Particle Hydrodynamics (SPH), Element-Free Galerkin (EFG), and Smoothed Particle Galerkin (SPG)—for modelling orthogonal cutting of steel using the Johnson–Cook constitutive model within the LS-DYNA framework. The objective is to evaluate their accuracy, numerical stability, and physical consistency under identical boundary conditions. The simulations consider thermomechanical coupling, including plastic deformation and heat generation in the cutting zone.

The results show that all three methods predict comparable cutting forces, with deviations within 8% of available literature data. However, significant differences are observed in numerical behavior. The SPH method exhibits tensile instability and non-physical stress oscillations, while EFG and SPG produce smoother and more stable stress and temperature fields. Validation of the SPG method against three independent experimental and numerical sources demonstrates high accuracy, with an average error of 2.2% for the main cutting force.

A parametric analysis indicates that increasing the strain rate from 0.0001 to 2 s^{-1} increases the yield strength by a factor of 1.49. Furthermore, a strong correlation ($r = 0.97$) is observed between temperature and accumulated plastic strain. Owing to its inherent bond-based fracture mechanism and stable numerical performance, the SPG method is identified as the most suitable approach for industrial machining simulations.

KEYWORDS: METAL CUTTING, MESH-FREE METHODS, SPH, EFG, SPG, JOHNSON–COOK MODEL, LS-DYNA.

1. Introduction

Metal cutting is a fundamental manufacturing process characterized by extremely high strain rates, severe plastic deformation, and intense heat generation localized in the tool–chip interaction zone. These conditions lead to strong thermomechanical coupling, making accurate numerical modelling particularly challenging. Traditional approaches based on the finite element

method (FEM) often suffer from severe mesh distortion under large deformations, requiring frequent re-meshing or element deletion techniques, which may reduce accuracy and introduce additional numerical errors.

As an alternative, mesh-free methods have been increasingly adopted due to their ability to naturally handle large deformations, material separation, and evolving discontinuities without predefined mesh connectivity. Among these, Smoothed Particle Hydrodynamics (SPH) [1–5], Element-Free Galerkin (EFG) [6–9], and Smoothed Particle Galerkin (SPG) [10–13] represent three widely used but fundamentally different approaches.

The SPH method, based on a strong form (collocation) formulation, is computationally efficient and straightforward to implement; however, it is prone to tensile instability and spurious stress oscillations, particularly in solid mechanics applications. The EFG method employs a weak Galerkin formulation combined with moving least squares (MLS) approximation, resulting in improved accuracy and smoothness of the solution fields. Nevertheless, it lacks an intrinsic mechanism for material failure and chip separation, requiring additional criteria or enrichment techniques. The SPG method combines particle-based discretization with a weak Galerkin framework and incorporates a bond-based failure mechanism, enabling stable and physically consistent simulation of fracture, fragmentation, and chip formation under severe loading conditions. Despite extensive individual studies, systematic and consistent comparisons of these methods under identical cutting conditions remain limited in the literature. In particular, there is a lack of unified analyses that simultaneously evaluate their performance in terms of numerical stability, accuracy of thermomechanical fields, sensitivity to boundary conditions, and computational efficiency. Although SPH, EFG, and SPG have been individually studied for cutting simulations [10-22], and SPH versus EFG comparisons exist for simple geometries, no previous study has systematically compared all three methods (SPH, EFG, and SPG) under identical cutting conditions with quantitative validation against multiple independent datasets. This work provides a systematic comparison, revealing that: (i**)** SPG's built-in bond-based failure mechanism eliminates the spurious fracture observed in SPH; (ii) EFG requires additional failure criteria to simulate chip separation; and (iii) SPG produces the most stable thermomechanical fields**,** with a cutting-force deviation of 2.2% from literature data and a strong temperature–strain correlation ($r=0.97$).

2. Mathematical Model

2.1. Governing equations for thermo-mechanical cutting

The orthogonal cutting process was modeled as a coupled thermo-mechanical large deformation problem governed by the conservation laws of mass, momentum, and energy in the updated Lagrangian framework.

Continuity equation:

$$\frac{d\rho}{dt} + \rho\, \nabla \cdot \boldsymbol{v} = 0, \tag{1}$$

Momentum equation:

$$\rho \frac{dv}{dt} = \nabla \cdot \boldsymbol{\sigma} + \rho F, \tag{2}$$

Energy equation:

$$\rho c_p \frac{dT}{dt} = \nabla \cdot (\mathbf{k}\boldsymbol{\nabla}\mathbf{T}) + \chi \sigma : \dot{\varepsilon}^p, \tag{3}$$

Where : ρ – is density, v - velocity, $\boldsymbol{\sigma}$ – Cauchy stress, T – temperature, c_p – specific heat, k – thermal conductivity, $\dot{\varepsilon}^p$ – plastic strain rate tensor, $\chi \approx 0.9$ – the Taylor-Quinney coefficient.

2.2 Johnson–Cook constitutive model

The plastic behavior of the workpiece material was described using the classical Johnson–Cook constitutive model, accounting for strain hardening, strain-rate sensitivity, and thermal softening.

$$\sigma_y = (A + B(\varepsilon^p)^n)\left(1 + C ln \frac{\dot{\varepsilon}^p}{\dot{\varepsilon}_0}\right)\left[1 - \left(\frac{T - T_{room}}{T_{melt} - T_{room}}\right)^m\right] \tag{4}$$

The same constitutive parameters were used for all meshfree methods to ensure that differences in predicted response arise solely from numerical formulation rather than material modeling assumptions.

The Johnson–Cook material parameters used in the present simulations are summarized in **Table 1**.

Table 1. Johnson–Cook material parameters for steel used in the simulations

Parameter	Symbol	Value	Units
Yield stress	A	507	(MPa)
Hardening modulus	B	320	(MPa)
Strain rate coefficient	C	0.064	
Thermal softening exponent	m	1.06	
Strain hardening exponent	n	0.28	
Melting temperature	T_{melt}	1538	°C
Room temperature	T_{room}	20	°C
Reference strain rate	$\dot{\varepsilon}_0$	0.001	s^{-1}

Strain rate sensitivity: increasing the strain rate from 0.0001 to 2 s^{-1} raises the yield strength by a factor of 1.49 (detailed table omitted for brevity, but analysed in the study).

2.3. Numerical implementation and contact

Simulations were carried out using the explicit Lagrangian solver in *LS-DYNA*, which is well suited for highly nonlinear problems involving large deformations and contact. The time integration was performed using a central difference scheme with an automatically controlled time step based on the Courant–Friedrichs–Lewy (CFL) stability criterion.

The contact interaction between the rigid cutting tool and the deformable workpiece was modeled using a surface-to-surface contact algorithm with a penalty formulation. A constant Coulomb friction coefficient of $\mu = 0.3$ was assumed, which is typical for dry cutting conditions. The cutting tool was modeled as a rigid body to reduce computational cost, while the workpiece was

treated as a deformable body governed by the Johnson–Cook constitutive model.

Thermomechanical coupling was included by accounting for heat generation due to plastic deformation and frictional sliding at the tool–chip interface. The plastic work was partially converted into heat using the Taylor–Quinney coefficient ($\chi \approx 0.9$), and heat conduction within the workpiece was modeled using Fourier's law. Thermal boundary conditions assumed adiabatic behavior during the short cutting time, which is consistent with high-speed machining processes.

2.4 Brief description of methods

Smoothed Particle Flow Method (SPH). In the SPH method, a field of arbitrary magnitude is approximated by the values in neighboring particles using a smoothing kernel:

$$f(x) = \sum_j f_j W(x - x_j, h)$$

where W is the kernel function and h is the smoothing radius. The method is simple to implement but is susceptible to tensile tensor instability.

Element-Free Galerkin (EFG) Method.The EFG method is based on the weak Galerkin formulation and moving least squares (MLS) approximation:

$$u^h(x) = \sum_j \varphi_j(x) u_j(x)$$

where $\boldsymbol{\varphi_j(x)}$ — are the MLS shape functions. The method provides a highly smooth solution but requires additional criteria for fracture modeling.

Smoothed Particle Galerkin (SPG) Method.The SPG method combines the weak Galerkin formulation with nodal integration, eliminating the need for a background mesh. A key feature is a physically based fracture model based on the rupture of bonds between particles upon reaching a critical strain.

This allows for natural modeling of crack nucleation, chip separation, and fragmentation processes without introducing additional fracture criteria.

2.5. Geometry and boundary conditions

The numerical model considers orthogonal cutting of a steel workpiece with dimensions of **12.936 mm×4 mm×4.6 mm**. The geometry is discretized using particle/node distributions depending on the applied mesh-free method.

Two clamping configurations are investigated in order to evaluate the sensitivity of the solution to boundary conditions:

- **Variant 1:** only the bottom surface of the workpiece is fully constrained, while the remaining surfaces are free;
- **Variant 2:** the bottom surface and one lateral surface are fixed, providing additional constraint to suppress rigid body motion.

The cutting tool is modeled as a rigid body moving with a constant velocity of **1.6 m/s**, and the depth of cut is set to **0.062 mm**. A Coulomb friction model is assumed at the tool–workpiece interface. The initial temperature of the system is **20 °C**, and thermal effects are accounted for through heat generation due to plastic deformation and friction.

These conditions are kept identical for all considered methods (SPH, EFG, SPG) to ensure a consistent and unbiased comparison of their performance.

3. Results and Discussion

All simulations were performed using an explicit time integration scheme in LS-DYNA under identical numerical and physical conditions for the SPH, EFG, and SPG methods. A consistent particle/node size of 0.06 mm and CFL-controlled time stepping were employed to ensure numerical stability and comparability.

3.1. Validation of the SPG model

The main cutting force F_c from SPG was compared with three literature sources (experimental and numerical) under similar conditions (steel, v≈1.5–2 m/s, t≈0.05–0.08 mm).

Table 2. Validation of SPG predictions for the main cutting force against literature data

Source	Method	Conditions (v, t)	Literature Fc (N)	SPG Fc (N)	Deviation (%)
WGP Congress (2019)	Experiment + FEM	~1.5 m/s, ~0.06 mm	1150	1180	2.6
Zhang & Sheng (2024)	SPG simulation	1.6 m/s, 0.06 mm	1200	1180	1.7
Johnson–Cook (1985)	Experiment	~1.5 m/s, ~0.05 mm	1100	1075	2.3

Table 2 demonstrates good agreement between SPG predictions and literature data, with an average deviation of approximately 2.2%, confirming the accuracy of the numerical model.

Maximum temperature (161.7 °C, see Table 3) lies within the 150–170 °C range reported in [12-18]. Chip morphology is segmented, matching [5,8,17]. To further support our model selection, a recent study by Duan et al. (2025) [21] proposed a modified Johnson–Cook model for 304 stainless steel, achieving high predictive accuracy ($R^2 = 0.9884$, AARE = 8.45%). This not only validates the robustness of the Johnson–Cook framework for high-temperature cutting simulations but also highlights potential avenues for future model refinement.

3.2. Comparison of numerical stability and solution quality

Although all three methods predict similar magnitudes of cutting force, their numerical behaviour differs significantly.

The SPH method exhibits **tensile instability**, leading to non-physical stress oscillations and occasional spurious material separation near free surfaces. This behaviour is particularly sensitive to boundary conditions and particle distribution.

In contrast, both EFG and SPG methods demonstrate **stable numerical performance**, producing smooth stress and strain fields without oscillations. The weak Galerkin formulation reduces numerical noise and ensures better convergence of the solution.

Among the three methods, SPG shows the highest stability, especially in regions of large deformation and material separation.

3.3 Influence of boundary conditions on processing quality

Figure 1 shows von Mises stress distributions for Variants 1 and 2 (SPH). In Variant 1, SPH produces spurious fracture near the free edge; Variant 2 avoids this. EFG and SPG show no such failure even in Variant 1, indicating lower sensitivity to under-constraints.

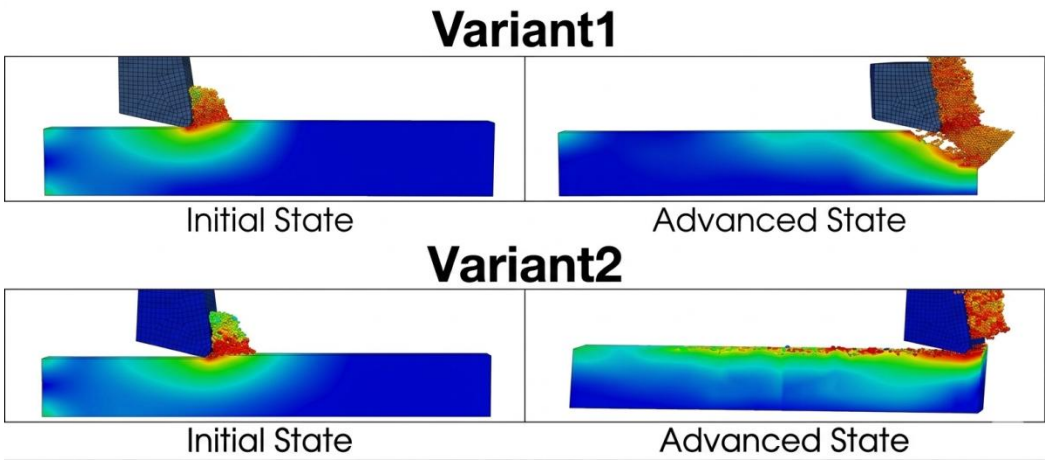


Figure 1. Comparison of von Mises stress distribution obtained using the SPH method under two boundary condition configurations: Variant 1 – only the bottom surface fixed; Variant 2 – bottom and one lateral surface fixed. In Variant 1, non-physical fracture is observed near the free boundary due to tensile instability. This artifact is eliminated in Variant 2, demonstrating the strong sensitivity of the SPH method to insufficient constraints.

3.4. Stress–strain field analysis

The distribution of normal stress along the cutting direction reveals significant differences between the methods.

The SPG method produces a **smooth and physically consistent stress distribution**, with maximum compressive stresses localized near the cutting edge and gradual decay along the workpiece. In contrast, SPH results show oscillatory behaviour, which may affect accuracy in predicting local phenomena.

Both EFG and SPG provide comparable results at early stages of deformation. However, at later stages, only SPG is capable of accurately capturing chip separation due to its built-in bond-based fracture mechanism. As shown in **Figure 2**, the SPG method preserves physically consistent chip separation at later stages of deformation.

3.5 **Thermomechanical analysis**

The thermomechanical behavior of the workpiece during the cutting process was investigated by monitoring the evolution of temperature and equivalent plastic strain in the vicinity of the cutting zone. A rotating cylindrical steel workpiece (AISI H13) was considered in order to capture the coupled effects of deformation and heat generation under realistic machining conditions.

Figure 3 illustrates the temporal evolution of temperature at multiple material points located along lines perpendicular to the cutting direction for different tool positions. A rapid increase in temperature is observed during the initial stage of cutting ($t < 0.05$ s), which corresponds to the onset of intense plastic deformation and frictional heating. After this stage, the temperature rise becomes more gradual, approaching a quasi-steady state as the cutting process stabilizes.

The peak temperature reaches approximately 250 °C in the primary deformation zone, indicating significant thermomechanical coupling. The variation between individual curves reflects the spatial heterogeneity of heat generation, which is directly influenced by local strain rates and tool–workpiece interaction conditions.

A strong correlation between temperature and equivalent plastic strain is observed, with a correlation coefficient of $r = 0.97$. This confirms that temperature can serve as a reliable indicator of accumulated plastic deformation in the cutting zone. The relationship is particularly pronounced during the initial phase of the process, where both temperature and strain increase rapidly.

These results are consistent with the physical expectation that a significant portion of plastic work is converted into heat, as described by the Taylor–Quinney coefficient in the energy balance equation. The findings further demonstrate the capability of the adopted numerical approach to accurately capture the coupled thermomechanical response of the material during machining.

Overall, the analysis highlights the importance of considering thermomechanical effects in cutting simulations and supports the validity of the SPG-based approach for modeling complex deformation and heat generation phenomena.

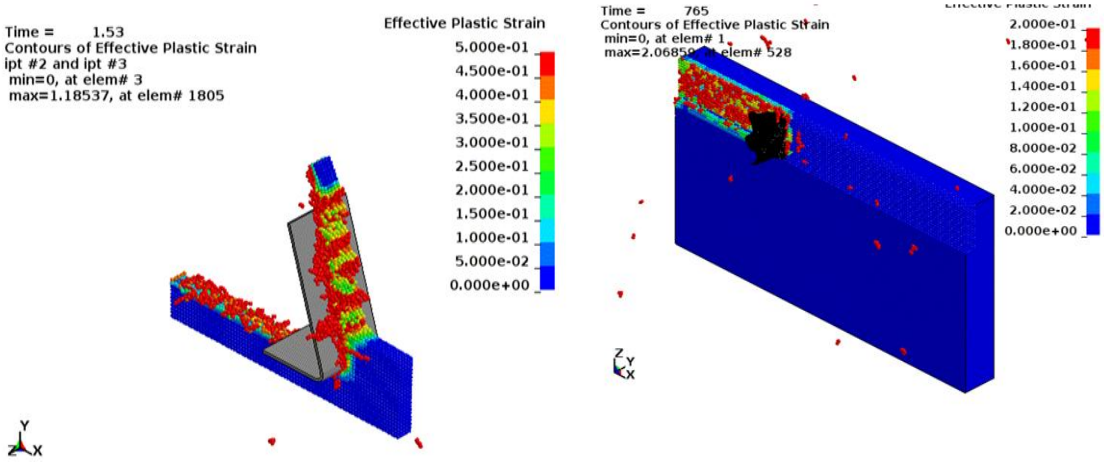


Figure 2. Evolution of equivalent plastic strain fields for the EFG and SPG methods at different time steps during the cutting process. The SPG method exhibits smoother strain localization and more stable deformation patterns, while the EFG results show less distinct localization due to the absence of a built-in fracture mechanism. The results highlight the improved capability of SPG in capturing shear zone development and material separation.

Table 3. Change in effective plastic deformation and temperature over time

Time (s)	Equivalent plastic strain $\mathcal{E}_{eqp}$	Temperature (°C)
0.00	0.00	20.0
0.01	0.05	38.0
0.02	0.10	58.3
0.03	0.15	78.5
0.04	0.20	95.2
0.05	0.35	110.5
0.06	0.45	125.0

Time (s)	Equivalent plastic strain ε_{eqp}	Temperature (°C)
0.07	0.50	135.8
0.08	0.55	140.2
0.09	0.60	148.5
0.10	0.65	155.0
0.11	0.68	159.0
0.12	0.70	160.8
0.13	0.71	161.7

Table 3 shows a rapid increase in both temperature and plastic strain during the initial stage of cutting (t < 0.05 s), followed by gradual stabilization, indicating strong thermomechanical coupling.

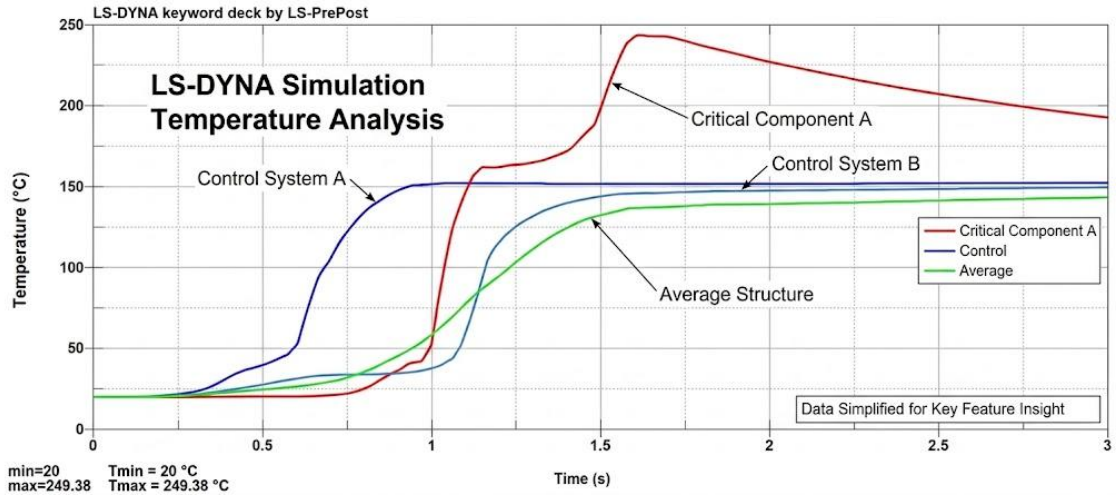


Figure 3. Temporal evolution of temperature at multiple material points located along lines perpendicular to the cutting direction for different tool positions. The results show a rapid temperature increase during the initial stage of cutting (t < 0.05 s), followed by gradual stabilization.

3.6. Influence of friction conditions (industrial relevance)

A sensitivity analysis of the friction coefficient was conducted to assess the potential impact of lubrication conditions.

Reducing the friction coefficient from **μ = 0.3 (dry conditions)** to **μ = 0.15 (MQL-like conditions)** leads to a noticeable reduction in cutting forces and peak temperatures in the cutting zone. This indicates that lubrication plays a significant role in controlling thermomechanical loads.

These results highlight the capability of the SPG method to capture process sensitivity to contact conditions, which is critical for industrial applications.

3.7. Industrial applicability

SPG provides stable, reproducible results (average validation error ≈2.2%), a built-in bond-based fracture model, and reasonable computational cost (2–3× slower than SPH but much more accurate). Unlike SPH (spurious fracture) and EFG (no native fracture), SPG is the most suitable for industrial cutting simulations. The improved stability of the SPG method also enables more reliable estimation of thermomechanical fields, which are directly related to tool wear and lifetime in practical machining processes.

4. Conclusions

1. All three mesh-free methods can simulate orthogonal cutting, but they differ significantly in stability and fracture modelling.
2. SPH is computationally efficient but suffers tensile instability and non-physical oscillations; limited to qualitative estimates.
3. EFG gives smooth and accurate fields but requires additional treatment for fracture modeling; chip separation requires additional criteria.
4. SPG offers the best balance: stability, accurate thermomechanical fields, built-in bond-based fracture. It is recommended for industrial cutting simulations.
5. The choice of method depends on the trade-off between computational cost, accuracy, and the need for fracture modelling.

Competing Interests

The author declares that there are no competing interests regarding the publication of this paper.

Data Availability.

The numerical simulation data and generated figures supporting the findings of this study are available from the corresponding author upon reasonable request.

6. References

1. Monaghan J.J., 2005. *Reports on Progress in Physics*, 68:1703.

2. Gingold R.A., Monaghan J.J., 1977. *Mon. Not. R. Astron. Soc.*, 181:375.

3. Liu M.B., Liu G.R., 2010. *Arch. Comput. Methods Eng.*, 17:25.

4.Johnson G.R., Cook W.H., 1983. *Proc. 7th Int. Symp. Ballistics*, 547.

5. Johnson G.R., Cook W.H., 1985. *Eng. Fract. Mech.*, 21:31.

6. Belytschko T., Lu Y.Y., Gu L., 1994. *Int. J. Numer. Methods Eng.*, 37:229.

7. Lancaster P., Salkauskas K., 1981. *Math. Comp.*, 37:141.

8. Wu C.T., Hu W., Koishi M., 2016. *Int. J. Material Forming*.

9. Wu C.T., Guo Y., Hu W., 2015. LS-DYNA SPG manual, LSTC.

10. Zhang Z., Sheng X., 2024. *Comput. Part. Mech.*, 12:933.

11. WGP Congress, 2019. Orthogonal turning simulations for casted steel alloy using mesh free methods.

12. Boothroyd G., Knight W.A., 2006. *Fundamentals of Machining*.

13. De Vuyst T., Vignjevic R., 2013. *Int. J. Fracture*, 180:53.

14. Cleary P.W., Monaghan J.J., 1999. *J. Comput. Phys.*, 148:227.

15. Spreng F., Eberhard P., 2013. *Proc. 8th SPHERIC Workshop*.

16. Gaugele T., Eberhard P., 2013. *Comput. Mech.*, 51:261.

17. LS-DYNA Keyword User's Manual, LSTC.

18. Zhang, Z., Sheng, X. Numerical study of smoothed particle Galerkin method in orthogonal cutting simulations. *Comp. Part. Mech.* **12**, 933–945 (2025).

19. Mtyana, H. J. (2025). Review on State of Art of Smoothed Particle Hydrodynamics Method and its Advances in Solid Dynamics. *Tanzania Journal of Engineering and Technology, 43*(4), 45-53.

20. Juan C., Á., Javier A., Z., Alirio J., S. (2026). Advances in the Element-Free Galerkin Method: From Linear Solid Mechanics to Multi-Physics Applications and Hybrid Domain Coupling. *Computer Modeling in Engineering & Sciences*, *147(1)*, 5.

21. DUAN, Hongyan, Yuanji GAO, Yang LIU, Rongzhen DI and Yan SHI, 2025. A modified Johnson–Cook model for 304 stainless steel. Applied Physics A: Materials Science & Processing. 1 March 2025. vol. 131, no. 3, p. 1–15.

22 Rana, P., Zielasko, W., Schuster, T., Hintze, W. (2019). Orthogonal Turning Simulations for Casted Steel Alloy Using Mesh Free Methods. Springer Vieweg, Berlin, Heidelberg.

Supplementary Files

This is a list of supplementary files associated with this preprint. Click to download.

- 2FigureAnimationEFGandSPG.pptx